Universiteit
Leiden
The Netherlands

Epigenetic alterations in the predisposition to and progression of melanoma

Salgado, C.

Citation
Salgado, C. (2020, October 21). *Epigenetic alterations in the predisposition to and progression of melanoma*. Retrieved from https://hdl.handle.net/1887/137852

Version:	Publisher's Version
License:	Licence agreement concerning inclusion of doctoral thesis in the Institutional Repository of the University of Leiden
Downloaded from:	https://hdl.handle.net/1887/137852

Note: To cite this publication please use the final published version (if applicable).

Cover Page

Universiteit Leiden

The handle http://hdl.handle.net/1887/137852 holds various files of this Leiden University dissertation.

Author: Salgado, C.
Title: Epigenetic alterations in the predisposition to and progression of melanoma
Issue date: 2020-10-21

4

Genome-wide characterization of 5-hydroxymethylcytosine in melanoma reveals major differences with nevus

Catarina Salgado, Jan Oosting, Bart Janssen, Rajiv Kumar, Nelleke Gruis, Remco van Doorn

Genes Chromosomes Cancer. 2020 Jun;59(6):366-374.

ABSTRACT

Melanoma demonstrates altered patterns of DNA methylation that are associated with genetic instability and transcriptional repression of numerous genes. Active DNA demethylation is mediated by TET enzymes that catalyze conversion of 5-methylcytosine (mC) to 5-hydroxymethylcytosine (hmC). Loss of hmC occurs in melanoma and correlates with disease progression. Here we analysed the genomic distribution of hmC along with mC in nevus and melanoma using oxidative bisulfite chemistry combined with high-density arrays. HmC was enriched relative to mC at enhancers, 5'UTR regions and CpG shores in nevus and melanoma samples, pointing to specific TET enzyme activity. The proportion of interrogated CpG sites with high hmC levels was lower in melanoma (0.54%) than in nevus (2.0%). Depletion of hmC in melanoma was evident across all chromosomes and intragenic regions, being more pronounced in metastatic than in non-metastatic tumours. The patterns of hmC distribution in melanoma samples differed significantly from those in nevus samples, exceeding differences in mC patterns. We identified specific CpG sites and regions with significantly lower hmC levels in melanoma than in nevus that might serve as diagnostic markers. Differentially hydroxymethylated regions localized to cancer-related genes, including the *PTEN* gene promoter, suggesting that deregulated DNA hydroxymethylation may contribute to melanoma pathogenesis.

KEYWORDS

5-hydroxymethylcytosine; DNA hydroxymethylation; DNA methylation; melanoma; *PTEN* gene

INTRODUCTION

Cutaneous melanoma is a malignant tumour derived from melanocytes residing in the skin. Clinically melanoma needs to be distinguished from melanocytic nevus, a benign lesion composed of melanocytes in a stable growth arrest.[1] Integrative genomic and transcriptomic analysis has identified common mutations and recurrent signaling perturbations yielding insight into melanoma biology.[2] In addition to accumulated genetic alterations, epigenetic mechanisms drive the development and evolution of melanoma.[3,4] DNA methylation, histone modifications and chromatin remodeling complexes regulate chromatin accessibility to transcription factors, thereby controlling gene expression programs. DNA methylation at CpG dinucleotides is mediated by DNA methyltransferases and additionally governed by DNA demethylation. Passive DNA demethylation can occur through insufficient methyltransferase activity during replication. Active demethylation involves the oxidation of 5-methylcytosine (mC) to 5-hydroxymethylcytosine (hmC) performed by the Ten Eleven Translocase (TET) family of dioxygenase enzymes.[5] In mammalian cells approximately 4% of all cytosines are methylated, and depending on cell type 0.1% - 0.7% of cytosine bases are hydroxymethylated.[6] Epigenetic deregulation is a universal characteristic of malignant tumours implicated in tumourigenesis. Cancer genomes are characterized by widespread loss of DNA methylation that contribute to genomic instability, and gain of DNA methylation at promoter CpG islands is associated with transcriptional repression.[7] In melanoma, selected tumour suppressor genes with a critical role in malignant transformation and metastatic behaviour, including *CDKN2A*, *PTEN* and *CDH11*, show frequent promoter hypermethylation and associated transcriptional silencing.[8] In addition, variation of methylation density at enhancer regions contributes to melanoma cell plasticity and correlates with patient survival.[9]

Different tumour types demonstrate loss of DNA hydroxymethylation and in certain instances this epigenetic event can be attributed to mutations in *TET* or *IDH* genes. Although the functional relevance of hmC loss remains to be resolved, studies in melanoma suggest its involvement in tumour progression.[10] Accordingly, low hmC levels were associated with worse survival from melanoma. Thus, in melanoma and other tumour types hmC loss might have diagnostic as well as prognostic significance. Hydroxymethylation mapping of melanoma samples using hydroxymethylated DNA immunoprecipitation showed hmC clusters in gene-rich regions and loss at specific loci.[10] In glioblastoma hmC depletion was shown to be most pronounced at enhancer regions.[11] To understand the functional consequences of aberrant hydroxymethylation and to apply it in the diagnosis and prognosis of melanoma, it is essential to obtain precise maps of the distribution of this epigenetic mark. Here we characterized the genomic distribution of hmC and mC in nevus and melanoma using oxidative bisulfite chemistry combined with arrays that simultaneously interrogate hmC

and mC at 850,000 CpG sites. This methodology is not affected by bias associated with antibody-based DNA capture methods and provides robust estimates of hmC and mC.[12] We sought to identify differentially hydroxymethylated CpG sites and regions by comparing nevus and melanoma hmC patterns. In addition, we compared the hmC patterns between primary melanoma samples that differ with respect to metastatic behavior. The genomic landscapes of hmC show depletion of hydroxymethylation in melanoma across various intragenic and intergenic regions compared to nevus. The hydroxymethylation patterns show more differences between nevus and melanoma than the methylation patterns, which has potential implications for biomarker discovery.

MATERIAL & METHODS

PATIENT SAMPLES

Fresh-frozen biopsy samples were obtained from patients diagnosed with common nevus (n=8), non-metastatic primary melanoma (n=8), and metastatic primary melanoma (n=8) (Supplementary Table S1). Only tissue samples containing at least 50% nevus or melanoma cells were included. Genomic DNA from all samples was extracted using the Genomic-tip kit (Qiagen, Hilden, Germany). The study was approved by the Leiden University Medical Center institutional ethical committee (05-036) and was conducted according to the Declaration of Helsinki Principles.

BISULFITE AND OXIDATIVE BISULFITE CONVERSION AND HYBRIDIZATION

Genomic DNA (1µg) was subjected to BS and OxBS conversion using the TrueMethyl 96 Kit (CEGX, Cambridge, UK) and applied to the Infinium MethylationEPIC BeadChip Kit (Illumina, San Diego, USA) at GenomeScan (Leiden, The Netherlands). The BeadChip images were scanned on the iScan system and the data quality was assessed using the R script MethylAid.[13]

850K BEADCHIP DATA ANALYSIS

Data were processed using the ChAMP package,[14,15] normalized using the default BMIQ algorithm and analysed as described previously with genome build GRCh37/hg19.[12] The ratio of the signal for the cytosine sequence to the combined intensity is the β-value, reflecting the methylation level on a scale from 0 (unmethylated) to 1 (fully methylated). To obtain the hydroxymethylation fraction oxBS β-values are subtracted from BS beta values, generating Δβ-values.[12,16] To define CpGs with high hmC we established a cut-off based on the average of absolute Δβ-value for all probes (0.008 plus 3 standard deviations, 0.166). To compare groups (nevus vs. melanoma; non-metastatic vs. metastatic melanoma) a statistical

test using the Limma R package[17] was used with multiple testing corrections applying a stringent p-value <0.005.[18] The Bump Hunting Algorithm was used to identify differentially hydroxymethylated regions with closely positioned probes.[19] The rate of hmC, the average of Δβ-values for a specific group of CpGs, was calculated according to intragenic location, to CpG-context regions and at enhancer regions (melanocytic cell-specific and general) retrieved from FANTOM5 project (http://FANTOM5.gsc.riken.jp/5/).[20]

VALIDATION OF CANDIDATE LOCI

Validation of hydroxymethylation at the *PTEN* promoter was performed in an independent sample group (4 nevi and 4 melanoma metastases). Genomic DNA (1μg) was subjected to BS and OxBS conversion using TrueMethyl oxBS Module (NuGEN Technologies, Redwood City, USA). DNA was amplified using the PCR_X Enhancer System (Thermo Fisher Scientific, Waltham, USA) and subjected to capillary sequenced (primers: GGGGTTGTAAATAGATTTGATAGG and AAAAATATCTCCTACTACAACCCAAAA) and deep paired-end sequencing (tailed primers: GATGTGTATAAGAGACAGGGGGTTGTAAATAGATTTGATAGG and CGTGTGCTCTTCCGATCTAAAAATATCTCCTACTACAACCCAAAA) using a MiSeq system (Illumina).

RESULTS

OBTAINING GENOME-WIDE 5-HYDROXYMETHYLCYTOSINE PATTERNS

Twenty-four DNA samples were analysed, including 8 aggressive primary melanomas with metastatic behaviour (M+), 8 primary melanomas with no metastatic behaviour (M-) during long-term follow-up and 8 benign nevi (N) (Table 1, Supplementary Table S1). To detect methylcytosine (mC) and hydroxymethylcytosine (hmC), different states of the CpG sites, we applied oxidative bisulfite (oxBS) chemistry, calculating hmC levels based on differences between bisulfite (BS) and oxBS-treated samples, using arrays as described previously.[11,12,21] Bisulfite (BS) converts unmethylated cytosines to uracil, while methylated and hydroxymethylated cytosines are protected. The prior oxidative step in oxBS conversion allows the distinction between methylated and hydroxymethylated cytosines. Only hydroxymethylated but not methylated cytosines are oxidated into formylcytosines (5fC), which are converted to uracil. Arrays that interrogate over 850,000 CpG sites representing 99% of the RefSeq genes, encompassing more than 90% of interrogated sites of 450K arrays plus 333,265 CpGs located at enhancer regions were used.[22] After quality control and exclusion of X-chromosomal CpGs 743,016 CpGs were analysed. As a measure of DNA methylation, the fluorescence ratio (β-value, ranging from 0 to 1) for each CpG of the bisulfite-treated DNA sample was used. Subtraction of the normalized β-value of the oxBS-treated sample from that of the BS-treated replicate analysed in parallel (Δβ-value)

was used as a measure of hydroxymethylation (Supplementary Figure S1). The average Δβ-value for CpGs at different genomic locations (hmC rate) was calculated. In addition, we considered as CpGs with high hmC levels those having a Δβ-value exceeding the average plus 3 standard deviations (Δβ>0.166).

TABLE 1. Clinical characteristics of nevus and melanoma samples subjected to genome-wide DNA (hydroxy)methylation analysis.

	Melanocytic Nevi n=8	Non-metastatic primary melanomas n=8	Metastatic primary melanomas n=8
Gender			
Female	6	4	4
Male	2	4	4
Age at diagnosis in years, median (range)	42 (29-57)	39 (34-68)	63 (45-79)
Location			
Head/neck	4	1	3
Trunk	2	4	2
Extremities	2	3	3
Breslow depth in mm, median (range)		1.0 (0.73-4)	9.7 (1.9-17)

First, we compared the number of hydroxymethylated CpGs in the nevus, non-metastatic and metastatic melanoma sample groups. The number of CpGs with high hmC levels was significantly higher in nevus (2.0% of interrogated CpGs) than in melanoma (0.54%) samples as was the average Δβ-value for the sample groups (0.017 vs 0.004), consistent with earlier reports of hmC loss in melanoma (Figure 1a)[10] Comparative analysis of melanoma and nevus samples revealed 21,767 CpGs with significantly lower hydroxymethylation in melanoma than in nevus samples, whereas 397 CpGs showed higher levels of hmC in melanoma (FDR <0.005). However, the variation of hmC levels of these CpGs within sample groups was high (Supplementary Figure S2). In spite of heterogeneity certain CpG sites showed consistent hmC loss in melanoma. The 50 most differentially hydroxymethylated CpGs are presented in a heatmap in Supplementary Figure S3. When comparing metastatic and non-metastatic primary melanoma samples there were no interrogated CpGs with statistically significant different hmC level.

To capture the distribution of hmC, principal component analysis revealed that the hmC patterns of melanoma samples were distinct from those of nevus samples (Figure 1b). The differences between the sample groups were more pronounced for hmC than for mC patterns. The hmC patterns of metastatic and non-metastatic melanoma samples were not distinct in this analysis. The hmC levels at different chromosomal regions were almost uniformly higher in nevus than in melanoma samples, with no evident clustering of aberrant hmC at specific chromosomal regions (Figure 1c).

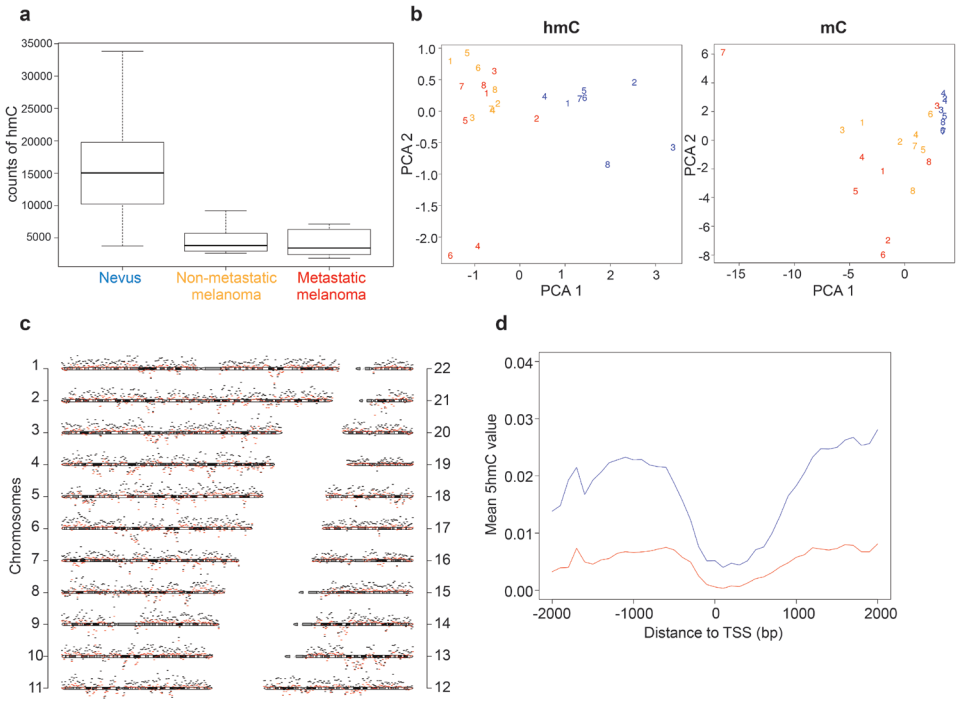

FIGURE 1. Genome-wide distribution of DNA hydroxymethylation in nevus, non-metastatic and metastatic melanoma. (a) Boxplot showing the counts of CpGs with high hmC (Δβ>0.166) for each group. (b) Principal component analysis of hmC and mC for 1% of probes with highest variation across samples. Numbers refer to individual samples. Blue – nevi; yellow – non-metastatic melanomas; red – metastatic melanomas. (c) Chromosomal distribution of hmC in nevi (black) and melanomas (red). The scheme of each chromosome represents the measurement baseline (null hmC level), the vertical distance between chromosomes is 10%, bin size is 1 Mb. (d) Mean of hmC level over 4 Kb around the transcription start sites for nevi (blue) and melanomas (red).

DEPLETION OF HMC IN DIFFERENT GENOMIC REGIONS

Since methylation of promoter, intragenic and intergenic regions has distinct associations with gene transcription, we determined the location of hmC and mC within these regions. First, we assessed the average hmC rate across 4Kb at promoter regions around the canonical transcription start site of all genes and observed slightly lower hmC levels in melanoma throughout the entire region compared to benign nevus (Figure 1d). TET proteins generate hmC as an intermediate from mC in active DNA demethylation; hmC levels tend to follow mC levels therefore. Accordingly, both mC and hmC levels were considerably lower at CpGs in the proximal promoter and first exon. However, the distal promoter (200-1500 bp upstream of transcription start site) and 5'UTR regions are exceptions that show high hmC

in spite of moderate mC levels in all sample groups (Figure 2a, b). Whereas the mC levels were only marginally lower in melanoma than in nevus, we observed a striking loss of hmC not only in promoters but across all gene regions. The levels of hmC were also significantly lower in the metastatic than in the non-metastatic melanomas in most gene regions.

Higher variation of hmC at enhancer regions in tumour has been reported in glioblastoma.[11] Therefore, we analysed the average rate of hmC at melanocyte-specific and at general enhancer regions retrieved from the FANTOM5 project.[20] We found higher hmC levels in enhancer compared to non-enhancer regions among the different sample groups (Supplementary Figure S4). The depletion of hmC at enhancer regions in melanoma compared with nevus was proportional to that at non-enhancer regions.

CpG islands, particularly located at promoter regions, are mostly protected from methylation. The regions adjacent to CpG islands, termed shores and shelves have also been found to demonstrate specific methylation patterns associated with transcriptional states.[23,24] Subsequently we calculated the hmC and mC levels of cytosines located in these regions and found that the mC levels were lower in CpG islands and shores than in shelves and open sea (Figure 2c, d). Again the loss of hmC in melanoma compared to nevus was much larger than the difference in mC across the CpG islands, shores, shelves and open sea. Whereas generally the hmC levels follow the mC levels, the CpG shores are another exception demonstrating high hmC in spite of moderate mC levels, especially in nevus samples.

Taken together, in nevus and melanoma hmC levels differ markedly across genomic regions and not following mC levels, which points to specific enzymatic activity in shaping hmC patterns. The hmC levels are substantially lower in melanoma than in nevus across all intragenic regions. This is in line with dilution through replication and insufficient active TET-mediated hydroxymethylation. Differences of hmC levels and distribution are much more pronounced than of mC levels.

DIFFERENTIALLY HYDROXYMETHYLATED REGIONS IN MELANOMA

Although the modification of a single CpG site may impact on gene expression, regions containing multiple CpG sites in promoters and enhancers commonly work as units of transcriptional regulation. Therefore, we sought to identify and examine regions with differential hydroxymethylation (DhMRs). When comparing melanoma and nevus samples, 68 regions were statistically significant differentially hydroxymethylated ($p<0.005$). In all 68 DhMR hmC levels were lower in melanoma compared to nevus (Figure 3, Supplementary Table S2). No significantly differentially hydroxymethylated regions were identified when comparing metastatic and non-metastatic melanoma samples. Five of these regions are located within

established cancer-related genes (http://cancer.sanger.ac.uk/census, accessed October 2019), namely in the *GNAS*, *GAS7*, *PTEN*, *TPM4* and *DAXX* (Supplementary Table S2). Notably, for the *PTEN* and *TPM4* tumour suppressor genes the DhMR is located in the promoter region.

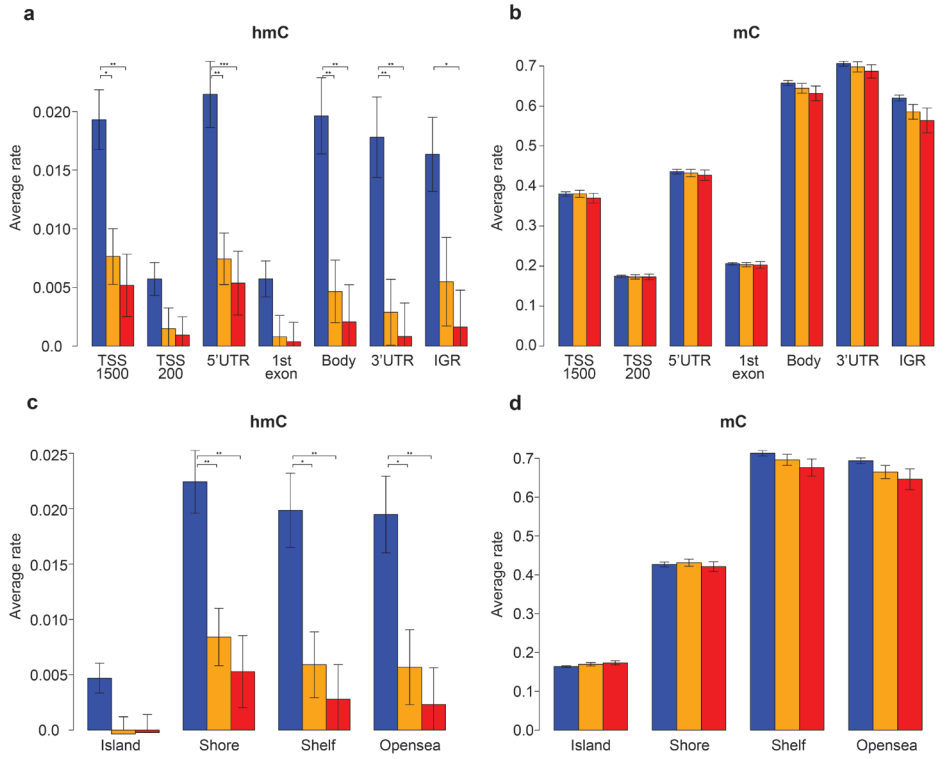

FIGURE 2. Average rate of hmC and mC at intragenic locations and CpG-context regions. (a) hmC levels in the N, M- and M+ sample groups at intragenic regions presented as average Δβ-values. (b) mC level presented as average β-values. Untranslated regions (3'UTR and 5'UTR), proximal promoter (TSS-200bp and 1stexon), distal promoter (TSS-1500bp), gene body, and intergenic region (IGR). (c) hmC levels in the N, M- and M+ sample groups at CpG-context regions presented as average Δβ-values. (d) mC level presented as average β-values. CpG island, shore (<2Kb flanking CpG Islands), shelves (<2Kb flanking outwards from CpG shore) and open sea (>4Kb from CpG island). Blue – nevi; yellow – non-metastatic melanomas; red – metastatic melanomas. The error bars represent standard errors among samples.

PTEN PROMOTER HYDROXYMETHYLATION IN NEVUS AND MELANOMA

PTEN is an established tumour suppressor gene, inactivated in melanoma and other tumour types through genetic and epigenetic mechanisms. Therefore, we further analysed hydroxymethylation at this locus in nevus and melanoma. In our study, a region in the *PTEN*

promoter (chr10:89621419-89622084) was found to show hydroxymethylation in all nevus samples, but higher methylation levels in the melanoma samples (Figure 4a).

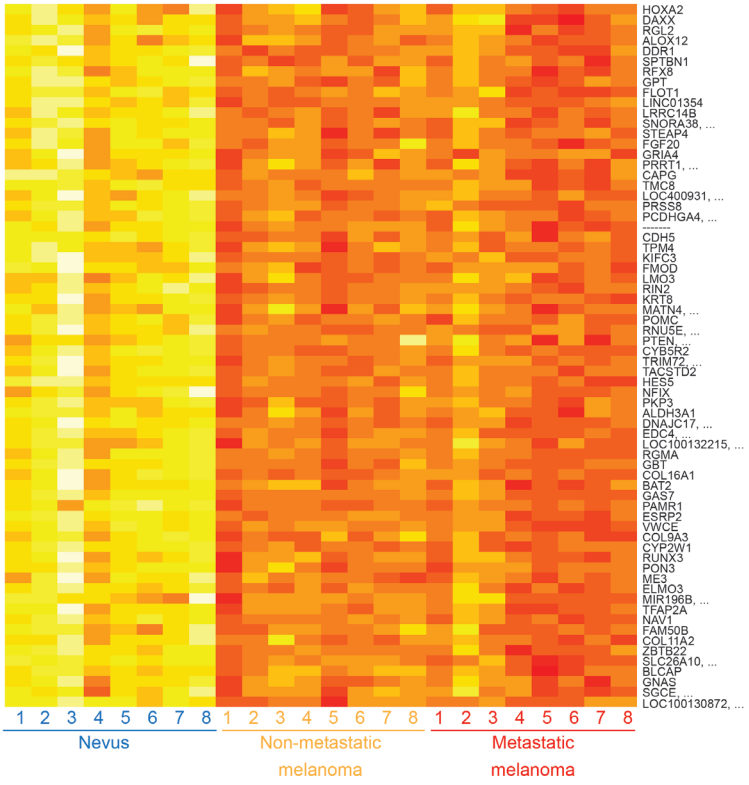

FIGURE 3. Heatmap depicting hmC levels for 68 significantly differentially hydroxymethylated regions in nevus and melanoma samples. Each row represents a DhMR with the associated gene and each column represents a different sample. Average hmC level, measured as Δβ-value, is indicated by variable colour (low hmC – red, high hmC – yellow).

Methylation of this specific region in the *PTEN* promoter, located from -1400 to -800bp upstream of the transcription start site, has been reported as being associated with transcriptional repression of *PTEN* in various malignancies and worse survival in melanoma patients (Supplementary Figure S5).[25-27] Capillary sequencing of the region following BS and oxBS conversion of DNA from nevus and melanoma samples subjected to hmC profiling, along with a normal skin sample, confirmed the presence of hydroxymethylation in nevus and normal skin samples (higher T peak upon oxBS) and methylation in a melanoma sample (maintenance of higher C peak after Bs and oxBS) (Figure 4b). Next, we analysed this DhMR

in the *PTEN* promoter using an independent quantitative BS/oxBS deep sequencing method in an independent set of 4 nevi and 4 metastatic melanoma samples. The 6 CpGs analysed using BS/oxBS NGS (chr10:89621419-89621537) confirmed the hydroxymethylation profile in nevi and a predominant methylation status in melanomas (Figure 4c).

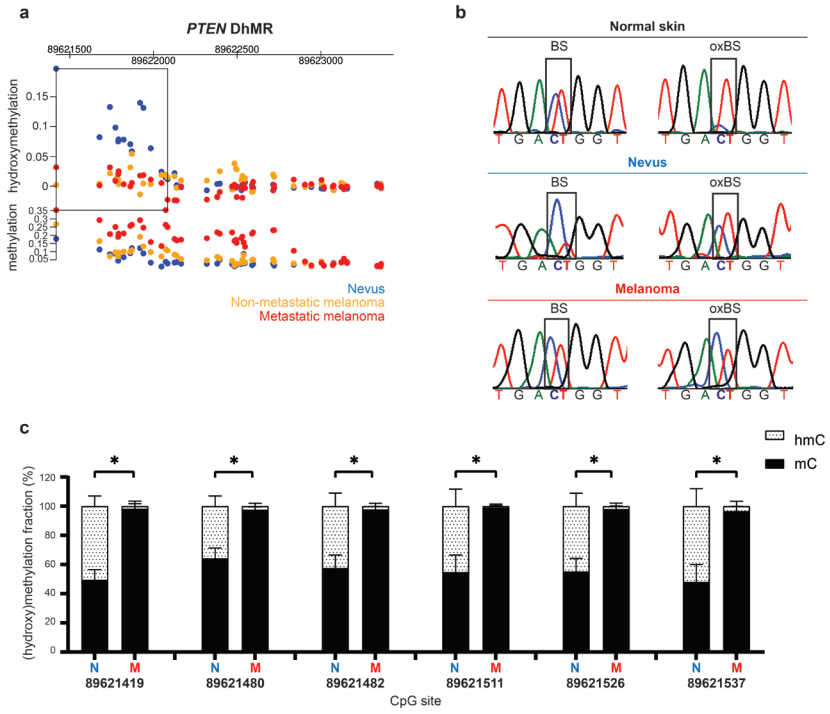

FIGURE 4. Differentially hydroxymethylated region in the *PTEN* promoter region. (a) DhMR (rectangle; chr10:89621419-89622084) located within the promoter region of *PTEN* gene with hydroxymethylation and methylation levels for the three sample groups. (b) Validation of a selected CpG site from *PTEN* DhMR by capillary sequencing upon BS and oxBS conversion. After oxBS a higher T peak appears in normal skin and nevus samples, while in melanoma sample there is a higher C peak. (c) BS/OxBS deep sequencing of 6 CpG sites at the *PTEN* DhMR (chr10:89621419-89621537) in 4 independent nevi and 4 melanomas (mean ± SD, *p<0.05, two-tailed Mann-Whitney U test). Blue – nevi; yellow – non-metastatic melanomas; red – metastatic melanomas.

DISCUSSION

Loss of hmC is an established feature of melanoma and other tumour types, with potential diagnostic and prognostic significance.[10,28] Here we provide a genome-wide landscape of hmC

and mC in nevus and melanoma by applying robust oxidative bisulfite chemistry combined with high-density arrays. Unsupervised analysis revealed significant differences in the global hmC patterns of melanoma and nevus samples, exceeding those of mC patterns. Numerous published studies have aimed to identify diagnostic and prognostic DNA methylation markers for melanoma.[29-31] Our study shows that analysis of hmC levels and distribution can equally be used to aid in distinguishing melanoma from benign melanocytic lesions. Accordingly, determination of hmC levels using immunohistochemistry in the diagnosis of melanoma has been proposed.[32] We identified thousands of single differentially hydroxymethylated CpG sites and 68 regions that might be used as specific diagnostic markers for melanoma. Although the levels of hmC were uniformly lower in metastatic than in non-metastatic melanoma, the patterns of distribution were not significantly different.

We observed a striking loss of hmC in melanoma relative to nevus, consistent with findings in other tumour types, across all autosomes, intragenic and intergenic regions, within and outside of CpG islands.[11,33] This phenomenon may be explained by passive dilution of the hmC mark due to DNA replication in proliferating melanoma cells and by insufficient active demethylation. Downregulation of IDH and TET family enzymes in melanoma has been shown previously, involving deregulation of active TET-mediated DNA demethylation in shaping the melanoma epigenome.[10] Within the pattern of global hmC depletion, specific CpG sites and regions could be identified with significantly lower hydroxymethylation in melanoma than in nevus, pointing to epigenetic deregulation at specific loci. In nevus and melanoma the hydroxymethylation levels were particularly low at the proximal promoter (TSS200) and first exon, corresponding with lower levels of methylation at promoter CpG islands. However, at CpG shores we observed high levels of hydroxymethylation disproportionate to the methylation levels at these sites in nevus and melanoma. Enrichment of hmC at CpG shores, regions that regulate gene expression, has been reported in non-small cell lung cancer and liver cancer previously.[24]

In melanoma and other tumour types, the methylation landscape demonstrates marked alterations at enhancer regions, which can impact on gene expression programmes and tumour aggressiveness.[9] Oxidation of mC into hmC is associated with enhancer activation.[34] Hydroxymethylation at these critical regulatory regions in tumours could induce functional demethylation and activation. In this study, we observed enrichment of hmC at enhancer regions in nevus and melanoma, as was reported for glioblastoma, but no excess depletion of hmC at enhancers in melanoma.[11]

The hmC mark is associated with an open chromatin configuration, affecting gene expression regulation.[34] Active demethylation can protect promoter and enhancer regions

from methylation-associated silencing. Loss of hmC might therefore contribute to malignant progression. Among the 68 DhMRs, 5 localized to the cancer-related genes *PTEN, DAXX*, *GAS7*, *GNAS* and *TPM4*. *PTEN* is an essential tumour suppressor gene in melanoma. Here, we demonstrate the presence of hydroxymethylation in the promoter region of the *PTEN* gene (chr10:89621419-89622084) in nevi and its absence in melanomas. It has been reported that *PTEN* expression is uniformly high in nevus and markedly lower in melanoma samples.[10,35,36] In melanomas, *PTEN* is functionally inactivated through genetic and epigenetic mechanisms, including promoter hypermethylation.[25,37] Loss of *PTEN* expression in murine nevi accelerates melanoma formation by allowing escape from oncogene-induced senescence.[38] It is tempting to speculate that hmC depletion at the *PTEN* regulatory region in melanoma has functional significance by affecting expression of this tumour suppressor gene. Accordingly, it was recently found that ablation of the *TET2* gene, resulting in genomic hmC loss, drives malignant transformation and melanoma progression.[39] In the genetically engineered mouse models studied deregulated expression of *CDKN2A* was observed. Even partial *PTEN* loss due to epigenetic mechanisms has biological relevance in melanoma.[36] Of note, the CpG sites showing hypermethylation in the study by Giles *et al.*[36] are located within the DhMR that we identified. The potential role of depletion of hmC at the *PTEN* promoter as an epigenetic mechanism driving melanoma progression requires further investigation.

In conclusion, we have resolved the genome-wide hmC and mC distribution in melanoma and nevus, of potential relevance for biomarker discovery and understanding of epigenetic deregulation in melanoma. We identified specific CpG sites and regions with significantly lower hydroxymethylation in melanoma than in nevus. Our results merit further investigation into the functional relevance of hydroxymethylation at the *PTEN* promoter in nevus and depletion at this locus in melanoma. Methods used in previous studies to analyse DNA methylation that rely on bisulfite conversion may have overestimated methylation, since part of the observed protection from conversion to uracil is caused by hydroxymethylation. However, we can assume that this potential error on melanoma is minor. Following on this genome-wide analysis of hmC, the value of the identified differentially hydroxymethylated CpG sites and regions should be tested in a large cohort of dysplastic melanocytic nevi and melanomas.

ACKNOWLEDGEMENTS

We thank AG Jochemsen and Mijke Visser for useful discussions, Leon Mei for bioinformatics support and Wim Zoutman and Coby Out (LUMC) for technical support. We thank Floor Pepers and Fahim Behrouz (GenomeScan) for help with genomic hmC mapping and validation. We acknowledge MELGEN, a Marie-Curie Consortium for all the scientific support.

REFERENCES

1. Damsky WE, Bosenberg M. Melanocytic nevi and melanoma: unraveling a complex relationship. *Oncogene.* 2017;36(42):5771-5792.
2. TCGA CGAN. Genomic Classification of Cutaneous Melanoma. *Cell.* 2015;161(7):1681-1696.
3. Fiziev P, Akdemir KC, Miller JP, et al. Systematic Epigenomic Analysis Reveals Chromatin States Associated with Melanoma Progression. *Cell reports.* 2017;19(4):875-889.
4. Lee JJ, Sholl LM, Lindeman NI, et al. Targeted next-generation sequencing reveals high frequency of mutations in epigenetic regulators across treatment-naive patient melanomas. *Clinical epigenetics.* 2015;7:59.
5. Tahiliani M, Koh KP, Shen Y, et al. Conversion of 5-methylcytosine to 5-hydroxymethylcytosine in mammalian DNA by MLL partner TET1. *Science.* 2009;324(5929):930-935.
6. Szwagierczak A, Bultmann S, Schmidt CS, Spada F, Leonhardt H. Sensitive enzymatic quantification of 5-hydroxymethylcytosine in genomic DNA. *Nucleic Acids Res.* 2010;38(19):e181.
7. Chen QW, Zhu XY, Li YY, Meng ZQ. Epigenetic regulation and cancer (review). . *Oncol Rep.* 2014;31(2):523-532.
8. Fu S, Wu H, Zhang H, Lian CG, Lu Q. DNA methylation/hydroxymethylation in melanoma. *Oncotarget.* 2017;8(44):78163-78173.
9. Bell RE, Golan T, Sheinboim D, et al. Enhancer methylation dynamics contribute to cancer plasticity and patient mortality. *Genome Res.* 2016;26(5):601-611.
10. Lian CG, Xu Y, Ceol C, et al. Loss of 5-hydroxymethylcytosine is an epigenetic hallmark of melanoma. *Cell.* 2012;150(6):1135-1146.
11. Johnson KC, Houseman EA, King JE, von Herrmann KM, Fadul CE, Christensen BC. 5-Hydroxymethylcytosine localizes to enhancer elements and is associated with survival in glioblastoma patients. *Nat Commun.* 2016;7:13177.
12. Stewart SK, Morris TJ, Guilhamon P, et al. oxBS-450K: a method for analysing hydroxymethylation using 450K BeadChips. *Methods.* 2015;72:9-15.
13. van Iterson M, Tobi EW, Slieker RC, et al. MethylAid: visual and interactive quality control of large Illumina 450k datasets. *Bioinformatics.* 2014;30(23):3435-3437.
14. Morris TJ, Butcher LM, Feber A, et al. ChAMP: 450k Chip Analysis Methylation Pipeline. *Bioinformatics.* 2014;30(3):428-430.
15. Fortin JP, Triche TJ, Jr., Hansen KD. Preprocessing, normalization and integration of the Illumina HumanMethylationEPIC array with minfi. *Bioinformatics.* 2017;33(4):558-560.
16. Field SF, Beraldi D, Bachman M, Stewart SK, Beck S, Balasubramanian S. Accurate measurement of 5-methylcytosine and 5-hydroxymethylcytosine in human cerebellum DNA by oxidative bisulfite on an array (OxBS-array). *PLoS One.* 2015;10(2):e0118202.
17. Ritchie ME, Phipson B, Wu D, et al. limma powers differential expression analyses for RNA-sequencing and microarray studies. *Nucleic Acids Res.* 2015;43(7):e47.
18. Benjamin DJ, Berger JO, Johannesson M, et al. Redefine statistical significance. *Nature Human Behaviour.* 2018;2(1):6-10.
19. Jaffe AE, Murakami P, Lee H, et al. Bump hunting to identify differentially methylated regions in epigenetic

epidemiology studies. *Int J Epidemiol.* 2012;41(1):200-209.

20. Lizio M, Harshbarger J, Shimoji H, et al. Gateways to the FANTOM5 promoter level mammalian expression atlas. *Genome Biol.* 2015;16:22.
21. Houseman EA, Johnson KC, Christensen BC. OxyBS: estimation of 5-methylcytosine and 5-hydroxymethylcytosine from tandem-treated oxidative bisulfite and bisulfite DNA. *Bioinformatics.* 2016;32(16):2505-2507.
22. Moran S, Arribas C, Esteller M. Validation of a DNA methylation microarray for 850,000 CpG sites of the human genome enriched in enhancer sequences. *Epigenomics.* 2016;8(3):389-399.
23. Irizarry RA, Ladd-Acosta C, Wen B, et al. The human colon cancer methylome shows similar hypo- and hypermethylation at conserved tissue-specific CpG island shores. *Nat Genet.* 2009;41(2):178-186.
24. Li X, Liu Y, Salz T, Hansen KD, Feinberg A. Whole-genome analysis of the methylome and hydroxymethylome in normal and malignant lung and liver. *Genome Res.* 2016;26(12):1730-1741.
25. Mirmohammadsadegh A, Marini A, Nambiar S, et al. Epigenetic silencing of the PTEN gene in melanoma. *Cancer research.* 2006;66(13):6546-6552.
26. Lahtz C, Stranzenbach R, Fiedler E, Helmbold P, Dammann RH. Methylation of PTEN as a prognostic factor in malignant melanoma of the skin. *The Journal of investigative dermatology.* 2010;130(2):620-622.
27. Roh MR, Gupta S, Park KH, et al. Promoter Methylation of PTEN Is a Significant Prognostic Factor in Melanoma Survival. *The Journal of investigative dermatology.* 2016;136(5):1002-1011.
28. Larson AR, Dresser KA, Zhan Q, et al. Loss of 5-hydroxymethylcytosine correlates with increasing morphologic dysplasia in melanocytic tumors. *Mod Pathol.* 2014;27(7):936-944.
29. Micevic G, Theodosakis N, Bosenberg M. Aberrant DNA methylation in melanoma: biomarker and therapeutic opportunities. *Clinical epigenetics.* 2017;9:34.
30. Wouters J, Vizoso M, Martinez-Cardus A, et al. Comprehensive DNA methylation study identifies novel progression-related and prognostic markers for cutaneous melanoma. *BMC medicine.* 2017;15(1):101.
31. Gao L, van den Hurk K, Moerkerk PTM, et al. Promoter CpG island hypermethylation in dysplastic nevus and melanoma: CLDN11 as an epigenetic biomarker for malignancy. *The Journal of investigative dermatology.* 2014;134(12):2957-2966.
32. Compton LA, Murphy GF, Lian CG. Diagnostic Immunohistochemistry in Cutaneous Neoplasia: An Update. *Dermatopathology (Basel, Switzerland).* 2015;2(1):15-42.
33. Haffner MC, Chaux A, Meeker AK, et al. Global 5-hydroxymethylcytosine content is significantly reduced in tissue stem/progenitor cell compartments and in human cancers. *Oncotarget.* 2011;2(8):627-637.
34. Mahe EA, Madigou T, Serandour AA, et al. Cytosine modifications modulate the chromatin architecture of transcriptional enhancers. *Genome Res.* 2017;27(6):947-958.
35. Tsao H, Mihm MC, Jr., Sheehan C. PTEN expression in normal skin, acquired melanocytic nevi, and cutaneous melanoma. *J Am Acad Dermatol.* 2003;49(5):865-872.
36. Giles KM, Rosenbaum BE, Berger M, et al. Revisiting the Clinical and Biologic Relevance of Partial PTEN Loss in Melanoma. *The Journal of investigative dermatology.* 2019;139(2):430-438.
37. Guldberg P, thor Straten P, Birck A, Ahrenkiel V, Kirkin AF, Zeuthen J. Disruption of the MMAC1/PTEN gene by deletion or mutation is a frequent event in malignant melanoma. *Cancer research.* 1997;57(17):3660-3663.

38. Vredeveld LC, Possik PA, Smit MA, et al. Abrogation of BRAFV600E-induced senescence by PI3K pathway activation contributes to melanomagenesis. *Genes Dev.* 2012;26(10):1055-1069.

39. Bonvin E, Radaelli E, Bizet M, et al. TET2-Dependent Hydroxymethylome Plasticity Reduces Melanoma Initiation and Progression. *Cancer research.* 2019;79(3):482-494.

SUPPLEMENTARY MATERIAL

SUPPLEMENTARY TABLE S1. Tumor samples characteristics.

Nr	Tumour type	Site	Breslow (mm)	Ulceration	Mitoses	Gender	Age	Color code
1	Naevus	leg				F	29	blue
2	Naevus	head & neck				F	52	blue
3	Naevus	trunk				F	43	blue
4	Naevus	upper leg				M	55	blue
5	Naevus	trunk				F	40	blue
6	Naevus	head & neck				F	39	blue
7	Naevus	head & neck				M	57	blue
8	Naevus	head & neck				F	30	blue
1	Met- primary melanoma	lower leg	2.08	yes	yes	M	68	orange
2	Met- primary melanoma	back	0.91	no	no	F	42	orange
3	Met- primary melanoma	foot	4	yes	yes	M		orange
4	Met- primary melanoma	buttock	0.73	no	no	F	35	orange
5	Met- primary melanoma	trunk	2.05	no	yes	F		orange
6	Met- primary melanoma	ear	0.81	no	yes	M	58	orange
7	Met- primary melanoma	shoulder	0.94	yes	yes	F	34	orange
8	Met- primary melanoma	back	1.06	no	yes	M	65	orange
1	Met+ primary melanoma	scalp	3.46	no	yes	M		red
2	Met+ primary melanoma	foot	1.9	no	yes	F		red
3	Met+ primary melanoma	back	3.09	no	yes	F	45	red
4	Met+ primary melanoma	neck, desmoplastic melanoma	15.6	no	yes	M		red
5	Met+ primary melanoma	thigh	9.2	yes	yes	F		red
6	Met+ primary melanoma	vulva	10.2	yes	yes	F	56	red
7	Met+ primary melanoma	scalp	17	yes	yes	M	79	red
8	Met+ primary melanoma	axilla	12	no	yes	M	70	red

Met- primary melanoma – non-metastatic primary melanoma

Met+ primary melanoma – metastatic primary melanoma

F – female

M – Male

SUPPLEMENTARY TABLE S2. 68 differentially hydroxymethylated regions (DhMRs).

Chr	start	end	p.valueArea	fwerArea	Gene ID
chr4	1201588	1203168	0.00E+00	0.00E+00	LOC100130872 LOC100130872-SPON2
chr7	94285642	94287211	0.00E+00	0.00E+00	SGCE PEG10
chr20	57462798	57464129	0.00E+00	0.00E+00	GNAS
chr20	36148133	36149455	0.00E+00	0.00E+00	BLCAP
chr12	58012960	58013942	0.00E+00	0.00E+00	SLC26A10 LOC101927583
chr6	33282885	33283317	0.00E+00	0.00E+00	ZBTB22
chr6	33130696	33132442	0.00E+00	0.00E+00	COL11A2
chr6	3848634	3849818	0.00E+00	0.00E+00	FAM50B
chr1	201708419	201709675	9.23E-06	8.00E-03	NAV1
chr6	10419016	10421069	1.85E-05	1.60E-02	TFAP2A
chr7	27208285	27209828	1.85E-05	1.60E-02	MIR196B HOXA10-AS
chr16	67232921	67234167	1.85E-05	1.60E-02	ELMO3
chr11	86382900	86383940	1.85E-05	1.60E-02	ME3
chr7	95025194	95027158	1.85E-05	1.60E-02	PON3
chr1	25257505	25258332	1.85E-05	1.60E-02	RUNX3
chr7	1022643	1023156	1.85E-05	1.60E-02	CYP2W1
chr20	61446962	61447623	1.85E-05	1.60E-02	COL9A3
chr11	61062665	61063378	1.85E-05	1.60E-02	VWCE
chr16	68270129	68271177	2.77E-05	2.40E-02	ESRP2
chr11	35546824	35548139	3.23E-05	2.80E-02	PAMR1
chr17	9862752	9863293	3.23E-05	2.80E-02	GAS7
chr6	31598379	31599955	3.23E-05	2.80E-02	BAT2
chr1	32169701	32170433	3.69E-05	3.20E-02	COL16A1
chr8	145728138	145728630	4.15E-05	3.60E-02	GPT
chr15	93616894	93617402	4.62E-05	4.00E-02	RGMA
chr2	63275509	63276833	5.08E-05	4.40E-02	LOC100132215 OTX1
chr16	67918001	67918965	5.08E-05	4.40E-02	EDC4 NRN1L
chr15	41061384	41062224	5.08E-05	4.40E-02	DNAJC17 C15orf62
chr17	19648846	19649293	5.08E-05	4.40E-02	ALDH3A1
chr11	392903	394545	5.08E-05	4.40E-02	PKP3
chr19	13135318	13135808	5.08E-05	4.40E-02	NFIX
chr1	2461278	2461929	5.08E-05	4.40E-02	HES5
chr1	59042931	59044110	5.08E-05	4.40E-02	TACSTD2
chr16	31227800	31228720	5.08E-05	4.40E-02	TRIM72 PYDC1
chr11	7695165	7695809	5.08E-05	4.40E-02	CYB5R2
chr10	89621419	89622084	5.08E-05	4.40E-02	PTEN KILLIN
chr5	80528581	80529340	5.08E-05	4.40E-02	RNU5E CKMT2
chr2	25391505	25391911	5.08E-05	4.40E-02	POMC
chr20	43936663	43937467	5.54E-05	4.40E-02	MATN4 RBPJL
chr12	53298383	53299310	5.54E-05	4.40E-02	KRT8
chr20	19866743	19867423	5.54E-05	4.40E-02	RIN2
chr12	16757954	16758465	6.92E-05	4.80E-02	LMO3
chr1	203320190	203320732	6.92E-05	4.80E-02	FMOD

Hydroxymethylation		Methylation			
Naevus	Melanoma	Naevus	Melanoma	In CpG island?	Cancer-related genes?[a]
0.09	-0.02	0.36	0.61	shore island	
0.02	-0.02	0.32	0.34	island shore	
0.04	-0.01	0.38	0.44	island shore	oncogene in pituitary adenoma, pancreatic intraductal papillary mucinous neoplasm, fibrous dysplasia
0.03	-0.01	0.81	0.77	island shore	
0.09	0.01	0.29	0.38	island shore	
0.10	0.00	0.35	0.50	island shore	
0.07	0.00	0.52	0.64	shore shelf	
0.05	0.00	0.25	0.38	island shore	
0.11	0.00	0.26	0.41	shore island	
0.07	-0.01	0.23	0.36	shore island	
0.05	-0.01	0.22	0.35	island shore	
0.13	0.00	0.34	0.54	island shore	
0.07	0.00	0.26	0.35	island shore	
0.03	-0.01	0.27	0.39	island shore	
0.08	0.01	0.30	0.47	island	
0.08	-0.03	0.42	0.59	shore	
0.10	0.02	0.23	0.27	shore	
0.11	0.00	0.31	0.41	island shore	
0.14	0.02	0.18	0.35	island	
0.09	0.00	0.29	0.38	island shore	
0.10	0.00	0.31	0.40	opensea	fusion partner in acute myeloid leukemia
0.04	0.01	0.80	0.86	shore island	
0.19	0.02	0.14	0.26	island shore	
0.13	-0.01	0.33	0.63	shore	
0.18	0.04	0.22	0.30	island shore	
0.04	-0.01	0.16	0.21	island	
0.10	0.00	0.42	0.60	shore island	
0.12	0.00	0.30	0.41	opensea	
0.07	-0.02	0.42	0.61	shore	
0.07	0.00	0.44	0.56	shore island	
0.12	0.01	0.10	0.20	island	
0.12	0.01	0.25	0.24	island	
0.08	0.00	0.17	0.22	island shore	
0.08	0.01	0.25	0.28	island shore	
0.12	0.00	0.21	0.33	island shore	
0.08	0.01	0.08	0.18	island shore	tumor suppressor gene in glioma, prostate, endometrial carcinomas
0.10	-0.01	0.37	0.51	opensea	
0.10	0.00	0.25	0.32	island shore	
0.02	-0.02	0.45	0.51	shore	
0.15	0.01	0.45	0.67	shore	
0.09	0.00	0.41	0.49	opensea	
0.10	0.00	0.20	0.24	opensea	
0.07	0.00	0.35	0.33	opensea	

SUPPLEMENTARY TABLE S2 CONTINUED.

Chr	start	end	p.valueArea	fwerArea	Gene ID
chr16	57831745	57832309	6.92E-05	4.80E-02	KIFC3
chr19	16178030	16178570	6.92E-05	4.80E-02	TPM4
chr16	66400320	66400599	6.92E-05	4.80E-02	CDH5
chr16	54972078	54973128	7.38E-05	4.80E-02	
chr5	140864020	140864834	7.38E-05	4.80E-02	PCDHGA4 PCDHGC4
chr16	31146682	31147199	7.38E-05	4.80E-02	PRSS8
chr22	46481603	46482023	7.38E-05	4.80E-02	LOC400931 MIRLET7BHG
chr17	76128481	76129099	7.38E-05	4.80E-02	TMC8
chr2	85640762	85641438	7.38E-05	4.80E-02	CAPG
chr6	32119616	32120324	7.38E-05	4.80E-02	PRRT1 PPT2
chr11	105479843	105480979	7.38E-05	4.80E-02	GRIA4
chr8	16859451	16860121	7.38E-05	4.80E-02	FGF20
chr7	87935979	87936923	7.38E-05	4.80E-02	STEAP4
chr6	31590513	31590736	7.38E-05	4.80E-02	SNORA38 BAT2
chr5	191127	192103	7.38E-05	4.80E-02	LRRC14B
chr1	234667087	234667549	7.38E-05	4.80E-02	LINC01354
chr6	30698584	30698987	7.38E-05	4.80E-02	FLOT1
chr8	145729106	145729799	7.38E-05	4.80E-02	GPT
chr2	102091048	102091755	7.38E-05	4.80E-02	RFX8
chr2	54785178	54785795	7.38E-05	4.80E-02	SPTBN1
chr6	30850309	30851086	7.85E-05	4.80E-02	DDR1
chr17	6898315	6899888	5.08E-05	4.40E-02	ALOX12
chr6	33263805	33265016	5.54E-05	4.40E-02	RGL2
chr6	33288366	33289280	4.62E-05	4.00E-02	DAXX
chr7	27142100	27143806	5.08E-05	4.40E-02	HOXA2

[a]Data retrieved from Cancer Gene Census - COSMIC (https://cancer.sanger.ac.uk/census)

Hydroxymethylation		Methylation			
Naevus	Melanoma	Naevus	Melanoma	In CpG island?	Cancer-related genes?[a]
0.08	0.00	0.43	0.65	shelf opensea	
0.05	-0.01	0.36	0.53	shore island	fusion partner in anaplastic large-cell lymphoma
0.08	-0.01	0.31	0.40	opensea	
0.10	0.00	0.31	0.30	island shore	
0.08	-0.01	0.26	0.29	island shore	
0.11	-0.01	0.36	0.55	opensea	
0.10	0.00	0.28	0.39	island shore	
0.21	0.04	0.28	0.38	shore	
0.04	-0.02	0.31	0.38	island shore	
0.11	0.01	0.35	0.46	shore	
0.07	0.00	0.28	0.32	shore	
0.12	0.01	0.28	0.36	shore island	
0.05	0.00	0.35	0.38	opensea	
0.11	0.02	0.36	0.53	shore	
0.05	0.01	0.23	0.31	island shore	
0.06	-0.04	0.30	0.59	opensea	
0.17	0.04	0.29	0.42	opensea	
0.06	-0.02	0.54	0.73	shore	
0.09	0.01	0.29	0.28	shore island	
0.08	0.00	0.11	0.20	island	
0.16	0.04	0.28	0.51	shore	
0.02	-0.03	0.37	0.57	island shore	
0.02	0.00	0.78	0.81	shelf shore	
0.02	-0.01	0.65	0.71	island shore	oncogene or tumor suppressor gene in pancreatic neuroendocrine tumour, paediatric glioblastoma
0.04	0.00	0.26	0.35	island shore	

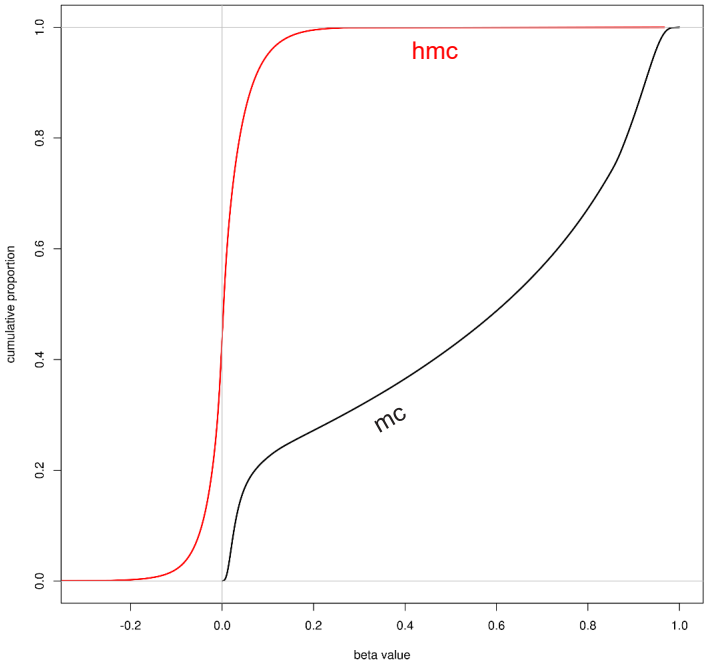

SUPPLEMENTARY FIGURE S1. Cumulative distribution of hmC and mC across all CpG sites analysed. Red line for hmC; black line for mC. All CpG sites show a hmC value between -0.2 and 0.3. The mC distribution is bimodal since there are non-methylated CpGs (0-0.2) or fully methylated CpGs (0.8-1).

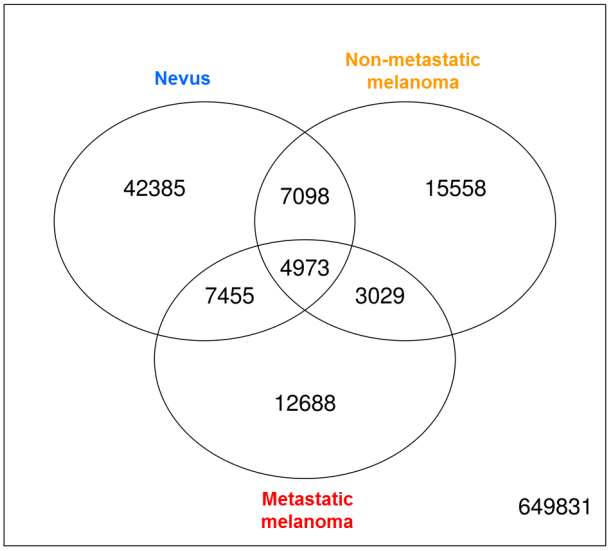

SUPPLEMENTARY FIGURE S2. Venn diagram of the GC-probes for which at least 1 sample within a group showed a Δβ value exceeding the average plus 3 standard deviations (Δβ>0.166).

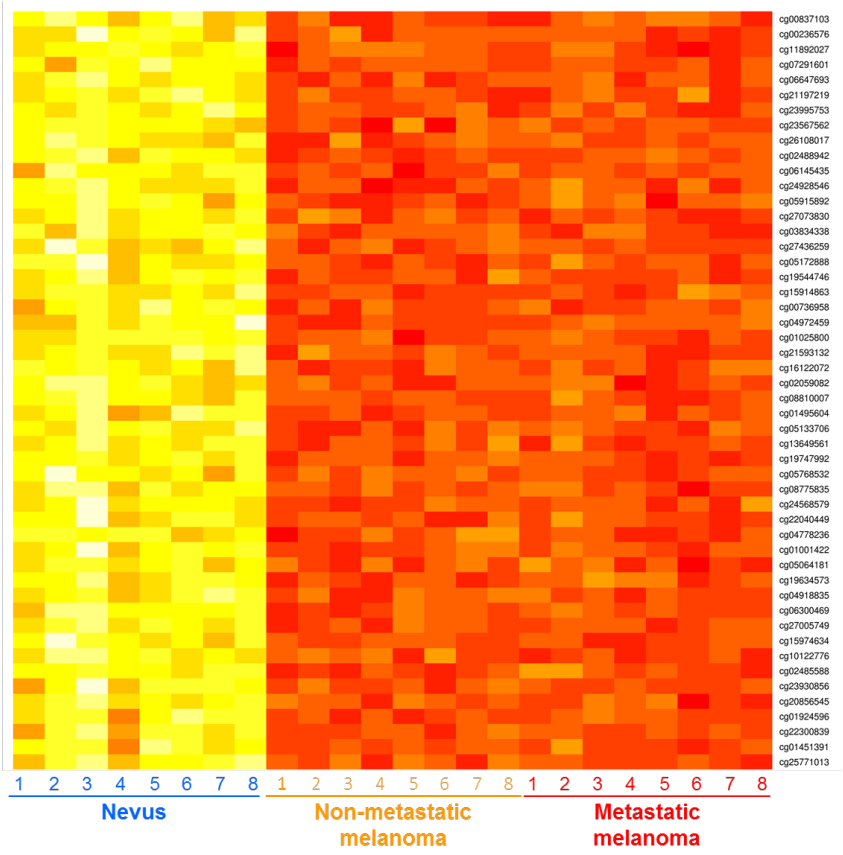

SUPPLEMENTARY FIGURE S3. Heatmap. The top50 CpG sites statistically significant between nevi and melanomas in order of hmC value.

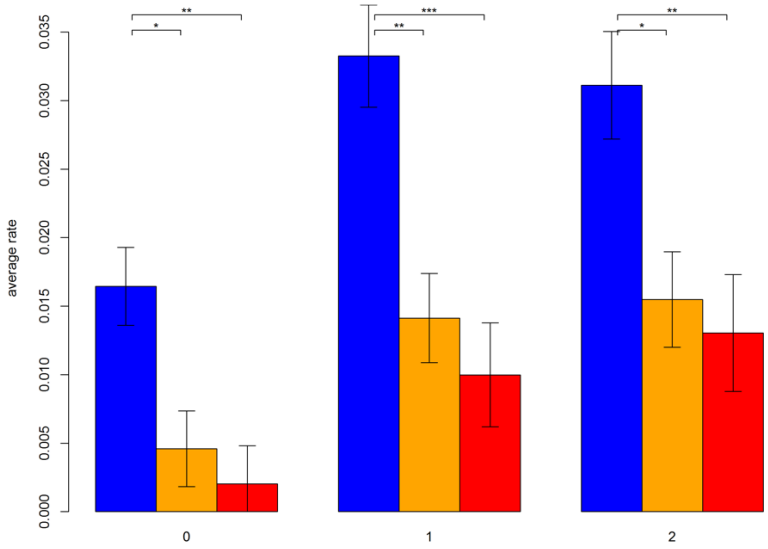

SUPPLEMENTARY FIGURE S4. Averaged rate of hmC at enhancer regions retrieved from FANTOM5 project (http://FANTOM5.gsc.riken.jp/5/). Blue – nevi; yellow – non-metastatic melanoma; red – metastatic melanoma. Comparison of hmC rate at melanocyte-specific enhancer regions (2) (2593 probes were found in 2136 enhancers) and at general enhancer regions (1) with hmC rate at non-enhancer regions (0).

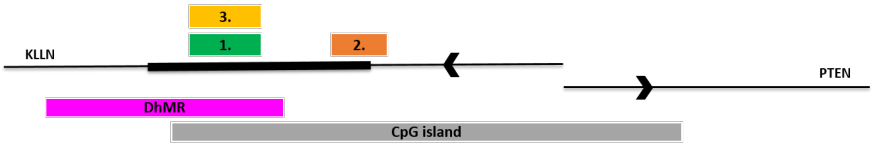

SUPPLEMENTARY FIGURE S5. Schematic representation of the DhMR in the *PTEN* promoter region (chr10:89621419-89622084). Hypermethylation of the regions 1. (Mirmohammadsadegh et al., 2006) and 2. (Lahtz et al., 2010) have been previously associated with transcriptional repression of the PTEN gene in melanoma. Hypermethylation of region 3. (Roh et al., 2016, same as region 1.) was associated with worse survival in melanoma patients.